

Article

Cleaner Production of Chromium Oxide from Low Fe(II)-Chromite

Qing Zhao ^{1,2,*}, Chengjun Liu ^{1,2}, Peiyang Shi ^{1,2} , Lifeng Sun ^{1,2}, Maofa Jiang ^{1,2}, Henrik Saxen ³  and Ron Zevenhoven ³

¹ Key Laboratory for Ecological Metallurgy of Multimetallic Mineral (Ministry of Education), Northeastern University, Shenyang 110819, China; liucj@smm.neu.edu.cn (C.L.); shipy@smm.neu.edu.cn (P.S.); sunlf@smm.neu.edu.cn (L.S.); jiangmf@smm.neu.edu.cn (M.J.)

² School of Metallurgy, Northeastern University, Shenyang 110819, China

³ Process and Systems Engineering Laboratory, Åbo Akademi University, 20500 Åbo/Turku, Finland; hsaxen@abo.fi (H.S.); rzevenho@abo.fi (R.Z.)

* Correspondence: zhaoq@smm.neu.edu.cn; Tel.: +86-024-8368-1478

Received: 14 April 2020; Accepted: 15 May 2020; Published: 19 May 2020



Abstract: Sulfuric acid-based leaching is a promising cleaner method to produce chromium salts, but its feasibility for treating low Fe(II)-chromite still remains to be proven. A Box–Behnken design (BBD)-based set of experiments for sulfuric acid leaching of low Fe(II)-chromite was utilized in this work for generating an experimental dataset for revealing the functional relationships between the processing parameters and the extraction yields of Cr and Fe. The dependent variables were found to exhibit strong intercorrelations and the models developed on the basis of statistical criteria showed excellent prediction accuracy. The optimum process conditions of leaching treatment were found to be a temperature of 176 °C, a dichromic acid/chromite mass ratio of 0.12, and a sulfuric acid concentration of 81%. Furthermore, the dissolution behavior of chromite in the leaching process and the effect of dichromic acid were experimentally investigated. It was found that the decomposition efficiency was highly dependent on the Fe(II) content of chromite, and that the dichromic acid acted both as an oxidant and a catalyst in the leaching process. On the basis of the results of this study, a novel process for treating low-Fe(II) chromite was proposed.

Keywords: mineral process; cleaner production; chromite; chromium oxide; hydrometallurgy

1. Introduction

Chromium (Cr) and its oxides have been widely applied in manufacturing tanning agents, pigments, stainless steel, alloys, and refractory materials [1–3]. As the primary natural source of Cr in nature, chromite consists of a series of spinel of Cr(III) oxide with magnesium oxide (MgO), aluminum oxide (Al₂O₃), and iron oxides (FeO and/or Fe₂O₃) [4]. More than 90% of the world's viable chromite reserves are found in South Africa, Kazakhstan, and Zimbabwe [5].

To extract the Cr for chromium salt preparation, researchers have proposed a leaching of the chromite using calcium, sodium, or potassium oxides/hydroxides in an oxidizing solvent solution [6–8]. In these processes, chromite decomposes caused by an oxidation of chromium from Cr(III) into Cr(VI) [9]. Bolaños-Benítez et al. [10] carried out a bio-leaching treatment of chromite tailings using *acidithiobacillus thiooxidans* (*A. thiooxidans*) and *pseudomonas putida*. Similar to the transformation route of alkali roasting, Cr(III) was initially oxidized and extracted in a hexavalent state, which was then reduced to a trivalent state by Fe and *A. thiooxidans*. *A. thiooxidans* has also been employed to remove Cr from tannery sludge [11] and soil [12].

The Cr(VI) has been proved to have toxic effects on organisms [13–15] and affect plant growth and development [16]. Therefore, governments are updating Cr regulations, and massive efforts have been

made on remediation of Cr-bearing wastes [17–22]. The dichromic acid generated in the remediation treatments is a kind of strong oxidant [23–25], which can be employed in mineral processing to promote ore decomposition.

To avoid the transformation from Cr(III) into Cr(VI) in the chromite processing, sulfuric acid leaching has been proposed and extensively studied [26–29]. In this process, Cr(III) is extracted from the chromite in a heated sulfuric acid solution with the help of recovered dichromic acid, with Cr(III) salts as products [30,31]. A lot of effort is presently being made to understand the dissolution behavior of chromite and improve the extraction yield of Cr. Researchers found that the extraction yield of high Fe(II)-chromite was always higher than that of low Fe(II)-chromite, and the reason was ascribed to the oxidation of ferrous into ferric iron in chromite [32–34]. The feasibility of the sulfuric acid leaching process on treating low Fe(II)-chromite has yet to be further evaluated, and the effect of the dichromic acid is still unclear.

With the aim of extracting Cr from low Fe(II)-chromite, sulfuric acid leaching treatment with the help of dichromic acid was investigated in the current work following an experimental plan, i.e., the Box–Behnken design (BBD), which is widely employed in different research fields to produce, in an optimal way, experimental data for response surface modeling [35–38]. By these methods, the combined effects of sulfuric acid concentration (*C*), dichromic acid/chromite ratio (*r*), and processing temperature (*T*) on the Cr and Fe extracting behavior were studied. Furthermore, three chromites with various Fe(II) contents were employed as comparison samples to investigate the dissolution behavior of chromite in the sulfuric acid-based leaching process.

2. Materials and Methods

2.1. Materials

Three chromites with various Fe(II) contents were studied in this work. Inductively coupled plasma-optical emission spectrometry (ICP-OES) and chemical analysis was performed to determine the chemical composition of the samples. Results are shown in Table 1, indicating the three chromites contained similar Cr₂O₃ content, and that the FeO contents in Zimbabwean chromite, Pakistani chromite, and South African chromite were about 1.5%, 6.7%, and 18.7%, respectively. On the basis of the FeO content, the three ores were referred to as low Fe(II)-chromite (LFC), medium Fe(II)-chromite (MFC), and high Fe(II)-chromite (HFC), respectively, in the current study. Furthermore, it was noted that the molar ratio between total bivalent metallic cations (Mg²⁺ + Fe²⁺) and total trivalent metallic cations (Cr³⁺ + Al³⁺ + Fe³⁺) in LFC was much lower than the theoretical ratio of a corresponding spinel (1:2). Molecular dynamics simulation of vacancy diffusion of chromite undertaken by Vaari [39] indicated that a bivalent metallic cation has a larger diffusion coefficient and a smaller activation energy for migration than other ions. Therefore, the low mole ratio between bivalent and trivalent metallics may be a sign of a crystal lattice defect of LFC.

The phase composition of samples was determined by X-ray diffraction (XRD), indicating the principal phases of the chromite were spinel and gangue (cf. Figure 1). Scanning electron microscopy-energy-dispersive X-ray spectroscopy (SEM-EDS) analysis using a Shimadzu SSX-550TM (Shimadzu Corp., Kyoto, Japan) showed that the gangue in chromite consists of a series of silicate species.

Dichromic acid prepared from the leachate of chromite ore processing residue was employed as an oxidant [31], while other reagents were purchased from Sinopharm Chemical Reagent Co., Ltd., Shanghai, China.

Table 1. Chemical composition (dry wt.%) of chromites.

Chromite	FeO	Fe ₂ O ₃	Cr ₂ O ₃	Al ₂ O ₃	MgO	SiO ₂	Other
Zimbabwean chromite (LFC)	1.52	21.56	45.95	12.05	6.40	2.80	9.72
Pakistani chromite (MFC)	6.67	5.34	42.29	13.01	19.75	6.67	6.27
South African chromite (HFC)	18.69	5.22	45.18	13.25	8.87	6.79	2.00

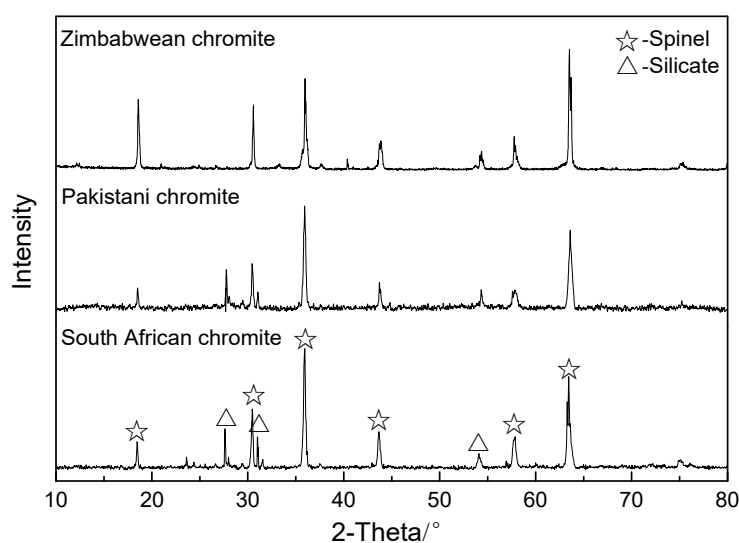


Figure 1. X-ray diffraction (XRD) patterns of chromites used in this study.

2.2. Methods

A certain amount of dichromic acid (dichromic acid/chromite ratio = 0.08, 0.10, and 0.12, respectively) and 150 mL sulfuric acid (sulfuric acid concentration = 70%, 80%, and 90%, respectively) was poured into an Erlenmeyer flask on an automatic temperature-controller electric heater. Ten grams of chromite powder (<74 μm) was added to the vessel when the solution heated to the set point (160, 180, and 200 $^{\circ}\text{C}$, respectively). After 60 min mechanical agitation, the leachate was removed from the heater and a filtration was carried out. The concentrations of metallic ions were determined by chemical analysis (for macro-elements) and ICP-OES analysis (for micro-elements), and the extraction yields of Cr and Fe (mass ratio between the filtrate and the chromite) were calculated. The Cr introduced from dichromic acid into the solution was deducted in the calculation of the extraction yield. After this, the effects of the processing temperature, dichromic acid/chromite ratio, and sulfuric acid concentration on the recovery behaviors of Cr and Fe were investigated.

2.3. Data Correlation Analysis Methods

The BBD was applied and quadratic response surface models were developed in the form

$$R_{\text{Cr}} = a_0 + a_1X_1 + a_2X_2 + a_3X_3 + a_{12}X_1X_2 + a_{13}X_1X_3 + a_{23}X_2X_3 + a_{11}X_1^2 + a_{22}X_2^2 + a_{33}X_3^2 \quad (1)$$

$$R_{\text{Fe}} = b_0 + b_1X_1 + b_2X_2 + b_3X_3 + b_{12}X_1X_2 + b_{13}X_1X_3 + b_{23}X_2X_3 + b_{11}X_1^2 + b_{22}X_2^2 + b_{33}X_3^2 \quad (2)$$

where R_{Cr} and R_{Fe} are the extraction yields (%) of Cr and Fe, respectively, a_0 and b_0 are constant terms in the models, a_i and b_i ($i = 1, 2, 3$) are the parameters of linear effect of the i th factor, a_{ij} and b_{ij} ($i, j = 1, 2, 3; i \neq j$) are the interaction effect parameters of the i th and j th factors, while a_{ii} and b_{ii} is the quadratic effect parameter of the i th factor. In Equations (1) and (2), X_1 , X_2 , and X_3 are the coded (dimensionless) factors of the original dependent variables (of sulfuric acid concentration in water C , dichromic acid/chromite ratio r , and temperature T) of the model, given by

$$X_1 = \frac{C - C_0}{\Delta C} \quad (3)$$

$$X_2 = \frac{r - r_0}{\Delta r} \quad (4)$$

$$X_3 = \frac{T - T_0}{\Delta T} \quad (5)$$

where C_0 , r_0 , and T_0 are the mid-values of the region, and ΔC , Δr , and ΔT are the intervals between the levels of the variables. This normalization yields variables that take on values -1 , 0 , or $+1$. On the basis of the thermodynamic analysis, the mid-values of C (80%, mass fraction), r (0.10), and T (180 °C) and the intervals (10%, 0.02, and 20 °C, respectively) were determined.

In order to test the statistical significance of parameters and evaluate the predictive ability of the models, analysis of variance (ANOVA) and multiple regression analysis were conducted, and the coefficient of determination (R^2), adjusted coefficient of determination (Adj. R^2) and predicted coefficient of determination (Pred. R^2) were calculated in this study. The 3D response surface plots were used to investigate the interactive effect of parameters on the extraction yields of Cr and Fe.

3. Results

3.1. Modeling

Table 2 shows the results of the BBD and the experimental extraction yields of Cr and Fe, $R_{Cr(\text{exp})}$ and $R_{Fe(\text{exp})}$, respectively.

Table 2. Box–Behnken design (BBD) with actual and coded values (in parentheses) for variables and experimental results.

Standard Order	Actual and Coded Level of Variables			$R_{Cr(\text{exp})}/\%$	$R_{Fe(\text{exp})}/\%$
	$C/\%$ (X_1)	$r/-$ (X_2)	$T/^\circ\text{C}$ (X_3)		
1	90 (+1)	0.10 (0)	160 (−1)	56.25	58.26
2	70 (−1)	0.08 (−1)	180 (0)	51.84	67.97
3	90 (+1)	0.10 (0)	200 (+1)	56.63	62.77
4	80 (0)	0.08 (−1)	200 (+1)	62.37	68.56
5	90 (+1)	0.12 (+1)	180 (0)	70.08	82.92
6	80 (0)	0.08 (−1)	160 (−1)	61.22	77.69
7	80 (0)	0.10 (0)	180 (0)	79.97	87.40
8	70 (−1)	0.10 (0)	200 (+1)	47.21	54.70
9	80 (0)	0.10 (0)	180 (0)	77.11	87.24
10	90 (+1)	0.08 (−1)	180 (0)	49.08	58.26
11	80 (0)	0.10 (0)	180 (0)	78.91	85.74
12	80 (0)	0.10 (0)	180 (0)	80.77	88.31
13	70 (−1)	0.10 (0)	160 (−1)	49.63	78.9
14	70 (−1)	0.12 (+1)	180 (0)	60.89	86.44
15	80 (0)	0.12 (+1)	160 (−1)	81.91	93.87
16	80 (0)	0.10 (0)	180 (0)	80.82	89.66
17	80 (0)	0.12 (+1)	200 (+1)	75.33	86.21

“-” means dimensionless.

Experimental results indicate that the sulfuric acid concentration (70–90%), dichromic acid/chromite ratio (0.08–0.12), and processing temperature (160–200 °C) have influence on the decomposition of chromite. It can be seen in Table 2 that the extraction yield of Cr falls in the range 50–80%, and it is always lower than that of Fe. Since the separation of Cr and Fe ions in solution is a challenge, the higher content of Fe in the leachate may cause problems in subsequent purification treatments. On the basis of the experimental results, the coefficients of the two polynomials can be defined by multiple regression analysis, and the Equations (1) and (2) can be expressed as

$$R_{Cr} = 79.52 + 2.81X_1 + 7.96X_2 - 0.93X_3 + 2.99X_1X_2 + 0.70X_1X_3 - 1.93X_2X_3 - 19.66X_1^2 - 1.88X_2^2 - 7.43X_3^2 \quad (6)$$

$$R_{Fe} = 87.67 - 3.22X_1 + 9.62X_2 - 4.56X_3 + 1.55X_1X_2 + 7.18X_1X_3 + 0.37X_2X_3 - 15.85X_1^2 + 2.08X_2^2 - 8.16X_3^2 \quad (7)$$

3.2. Model Validation

ANOVA was used to test the statistical significance of the parameters of the Response surface methodology (RSM) quadratic model, with results listed in Table 3. For the model of Cr, the resulting $F = 83.70$ suggests that the model is clearly significant, with only a 0.01% chance that such a value could occur by chance. Values of probability $> F$ lower than 0.05 means that the terms of model are significant, while values exceeding 0.10 indicate the terms are not significant for the model. According to this, the terms C , r , Cr , C^2 and T^2 are significant, and terms T , CT , rT , and R^2 are not significant. For the model of Fe, the resulting $F = 100.07$ indicates significance, just as for the Cr model. Significant terms in this model are C , r , T , CT , C^2 , r^2 , and T^2 , and the other terms are not.

Table 3. ANOVA for response surface methodology (RSM) quadratic models developed.

Source	Cr					Fe				
	Sum of Square	df	Mean Square	F Value	p-Value Prob. > F	Sum of Square	df	Mean Square	F Value	p-Value Prob. > F
Model	2608.23	9	289.80	83.70	<0.0001	2607.88	9	289.76	100.07	<0.0001
C	63.11	1	63.11	18.23	0.0037	83.21	1	83.21	28.73	0.0011
r	507.21	1	507.21	146.50	<0.0001	740.36	1	740.36	255.68	<0.0001
T	6.98	1	6.98	2.01	0.1988	166.35	1	166.35	57.45	0.0001
Cr	35.70	1	35.70	10.31	0.0148	9.58	1	9.58	3.31	0.1118
CT	1.96	1	1.96	0.57	0.4763	206.07	1	206.07	71.16	<0.0001
rT	14.94	1	14.94	4.31	0.0764	0.54	1	0.54	0.19	0.6788
C ²	1627.52	1	1627.52	470.08	<0.0001	1057.61	1	1057.61	365.25	<0.0001
r ²	14.93	1	14.93	4.31	0.0765	18.15	1	18.15	6.27	0.0408
T ²	232.16	1	232.16	67.06	<0.0001	280.62	1	280.62	96.91	<0.0001

Detailed descriptive statistical performance indices for the proposed models are shown in Table 4. R^2 , Adj. R^2 , and Pred. R^2 were used to evaluate the predictive ability and the goodness of fit of the model, and the results are listed in Table 4 as well. The high values of the coefficient of determination for Cr and Fe imply that only 1% of the total variations cannot be explained by Equations (6) and (7), meaning the dependent variable shows a strong correlation with the independent variables. The Adj. R^2 is usually employed to compare the explanatory power of regression models, which shows high values for the Cr and Fe models in this work. Pred. R^2 was calculated to test how well the model predicts responses for new observations. For both models, the differences between Pred. R^2 and Adj. R^2 < 0.1 implying that Pred. R^2 coincides well with the Adj. R^2 [40].

Table 4. Detailed descriptive statistical regression analysis for the models.

Element	Standard Deviation	Mean	Coefficient of Variance (C.V.%)	R^2	Adj. R^2	Pred. R^2
Cr	1.86	65.88	2.82	0.9908	0.9790	0.9055
Fe	1.70	77.35	2.20	0.9923	0.9824	0.9225

The predicted extraction yields calculated by Equations (6) and (7) and the experimental values are shown in Figure 2. The data points fall close to the 45° line, meaning that the proposed models can accurately predict the leaching yields of Cr and Fe in sulfuric acid-based leaching operated under the conditions studied.

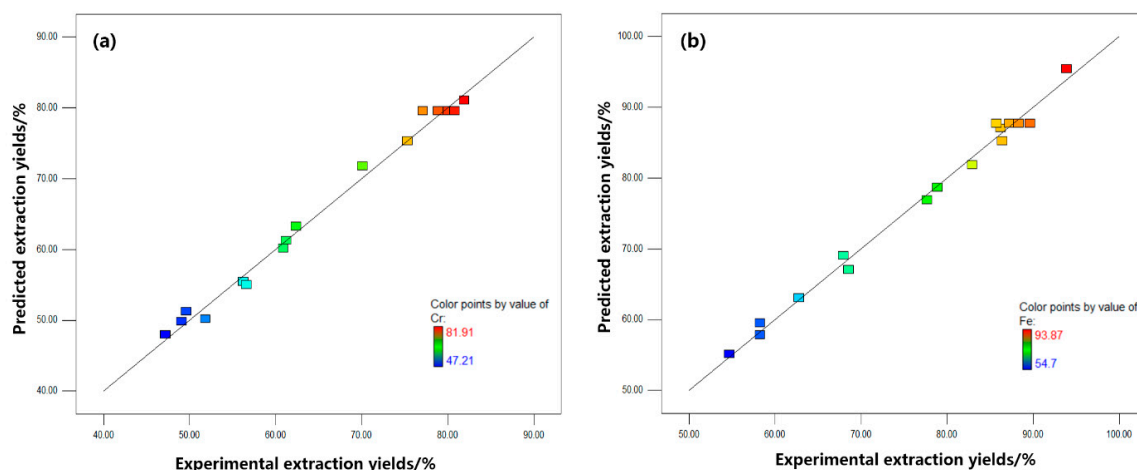


Figure 2. Relationships between experimental and predicted extraction yields of (a) Cr and (b) Fe.

3.3. Optimization

Three-dimensional response surface plots are helpful tools to investigate the overall and coupled effects of the inputs on the outputs for the LFC sample. Figure 3 shows the plots of two parameters determining the extraction yields by keeping the other variable at a certain value, and the optimum conditions for the sulfuric acid leaching of LFC can be easily identified. It can be seen in Figure 3 that the extraction yields of Cr and Fe exhibit similar trends with respect to the inputs. The leaching efficiency significantly increased with the dichromic acid dosage in the current work. The plots of extraction yield versus solution acidity and temperature show a parabolic dependence, indicating that reasonable sulfuric acid concentration and temperature would be around 80% and 180 °C. Elevation of acidity and temperature to a higher-level lead to a decrease in the recovery of Cr and Fe while more solid residues were obtained.

It was noted that the color of the leaching residues changed from light gray to green when the temperature elevated from 160 to 200 °C. Other researchers have observed the same in sulfuric acid-based processing of chromite, and the results indicate that the green residues were mixed Cr-bearing sulfates [27,33,34]. The precipitation of these sulfates is attributed to the local supersaturation induced by a rapid dissolution and high viscosity of the solution in the concentrated sulfuric acid at such a high temperature. The mixed sulfates precipitated and covered the chromite particles, inhibiting further decomposition of the ore. Furthermore, the trivalent state of chromium in sulfate could be easily oxidized to the toxic hexavalent state, making the residue become a potential source of chromium contamination. Therefore, these sulfate phases should be prevented from precipitating by controlling processing parameters or recovered via some specific methods.

To optimize the leaching treatment of chromite with respect to the Cr recovery, Derringer's desirability function was employed in the studied range. Results exhibited a maximum value of $R_{Cr} = 86.3\%$ when the sulfuric acid leaching process is carried out at 176 °C with a sulfuric acid concentration of 81% and dichromic acid/chromite ratio of 0.12. In order to confirm this finding, the duplicate confirmatory tests were conducted under these conditions and the extraction yield of Cr was found to be 84.2%, demonstrating the proposed model has a good predictive ability for treating this chromite. Some SEM images of the LFC before and after leaching under the optimum conditions are shown in Figure 4. As seen in this figure, the particle size of the ore significantly decreased after the leaching treatment. Corrosion was found to occur on the surface of the spinel particles, giving the particles a rough surface. Unreacted chromite was the only phase that can be detected in the leaching residue, which can be recycled and used in further leaching process.

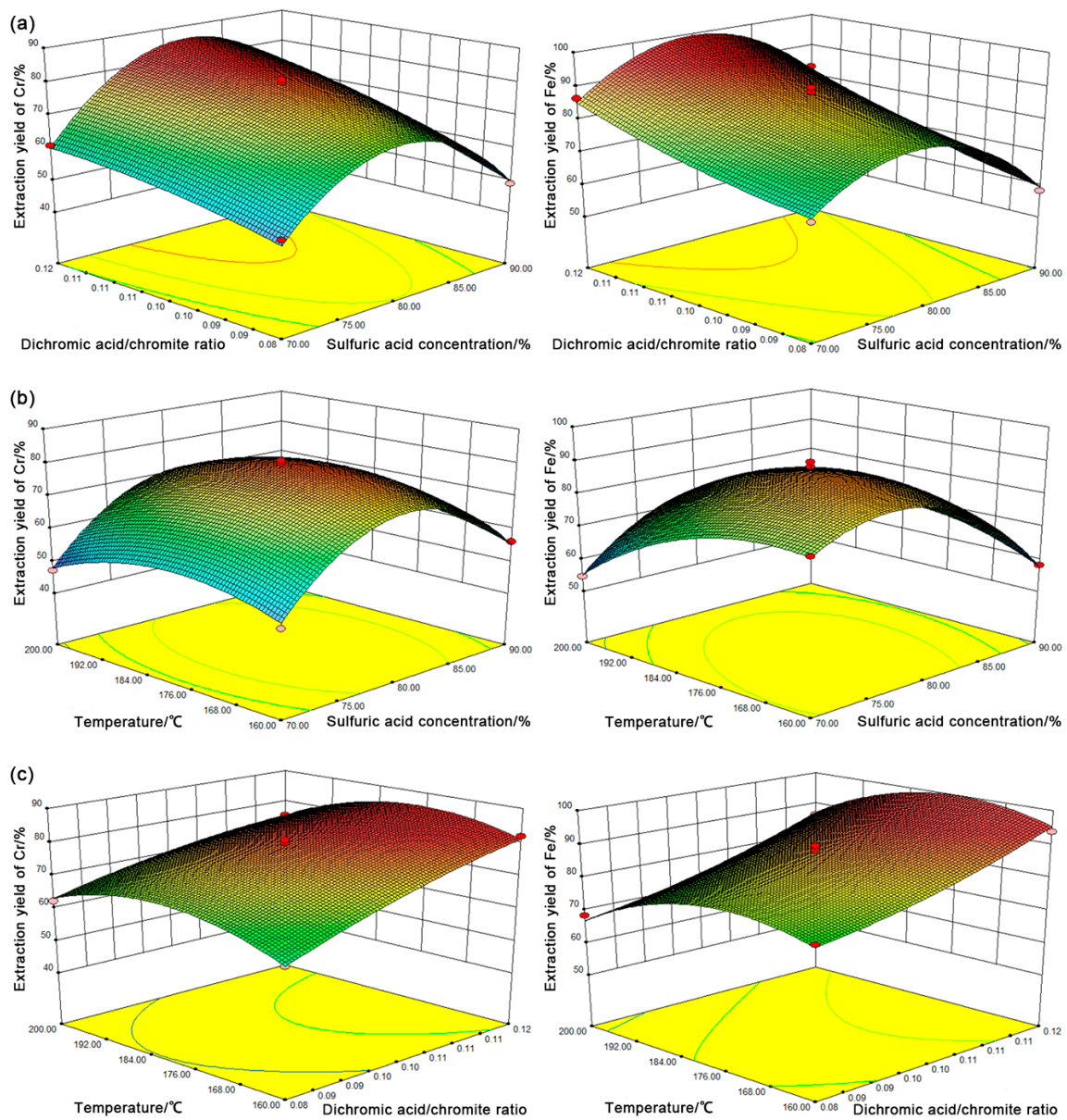


Figure 3. Three-dimensional response surfaces of extraction yield as a function of (a) sulfuric acid concentration and dichromic acid/chromite ratio at a temperature of 180 °C; (b) sulfuric acid concentration and temperature for a dichromic acid/chromite ratio of 0.10; (c) dichromic acid/chromite ratio and temperature for a sulfuric acid concentration of 80%.

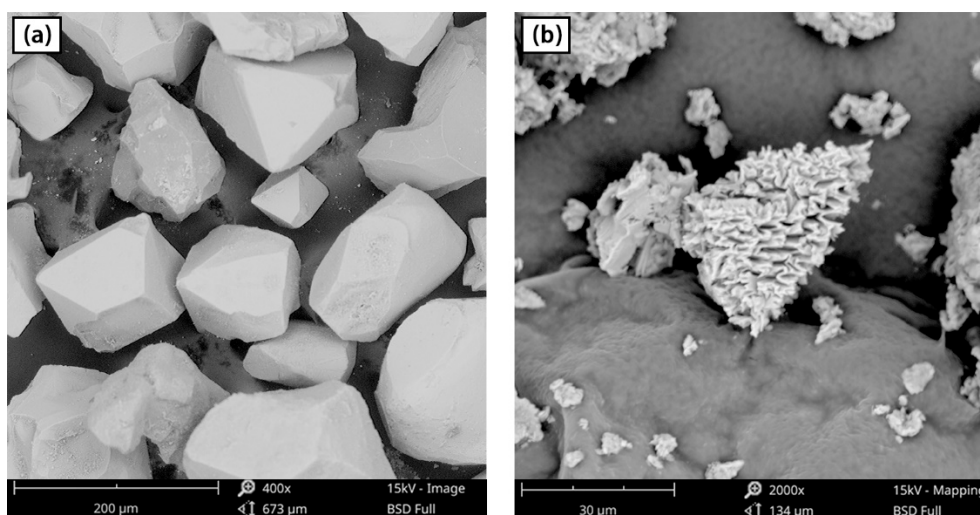


Figure 4. Scanning electron microscopy (SEM) images of low Fe(II)-chromite (LFC) (a) before and (b) after leaching at 176 °C with a sulfuric acid concentration of 81% and dichromic acid/chromite ratio of 0.12.

3.4. Effect of Dichromic Acid

On the basis of the obtained results, the decomposition efficiency of chromite in sulfuric acid-based solution seems closely associated with the oxidation potential of the solution. Inspired by these findings, three chromites with different contents of Fe(II) (LFC, MFC, and HFC) were used to investigate the dissolution behavior of chromite and the effect of dichromic acid. With the goal to avoid the interference effect of mixed Cr-bearing sulfates, a series of exploratory experiments was first conducted for the three ores. The results indicate that little sulfate was detected when the leaching treatment was performed at 160 °C for 60 min at a sulfuric acid concentration of 80% and dichromic acid/chromite ratio of 0.08. Therefore, these conditions were selected for investigating the chromite decomposition mechanism. A series of dichromic acid-free leaching tests were carried out as well. Figure 5 shows the extraction yields of Cr of the different chromites and final Cr(VI) concentrations in the leachates.

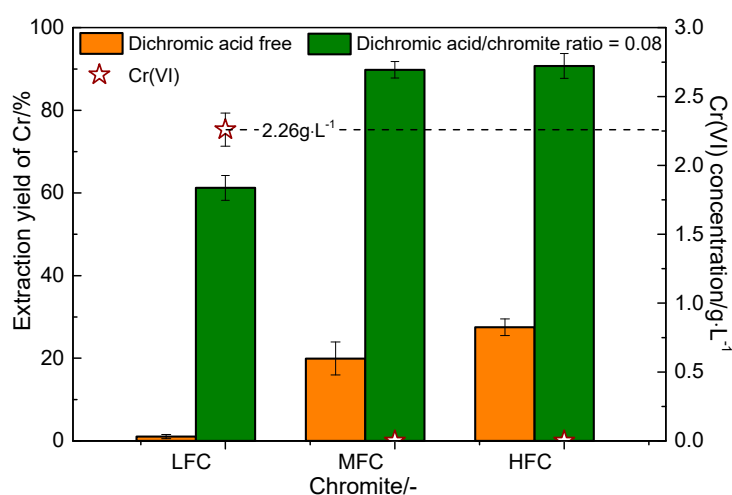


Figure 5. Extraction yields of Cr of different chromites and final Cr(VI) concentrations in the leachates.

As seen in Figure 5, chromites of different Fe(II) contents give rise to different results under the same leaching condition. In the dichromic acid-free tests, more than 20% of the Cr was extracted from MFC and HFC, while LFC hardly decomposed in the 80% sulfuric acid solution at 160 °C, demonstrating its higher stability. When using an oxidizing solution, such as the sulfuric acid solution used here,

to dissolve the spinel phase, some Fe(II) in spinel transforms into Fe(III) generating a decrease of ionic radius, so the lattice distortion of crystal structure occurs. This promotes the chromite decomposition in acid solutions, which explains why it is much easier to dissolve high Fe(II)-chromite than that with low Fe(II) content. Moreover, Vaari [39] has proposed that the diffusion coefficient of Fe^{2+} are much larger compared with that of other metallic ions in spinel. In the oxidizing atmosphere, Fe^{2+} ions tend to migrate from the core of spinel crystals toward the reaction interface and are oxidized into Fe^{3+} producing tetrahedral vacancies [41,42]. Hydrogen ions provided by the acid attack the oxygen skeleton of the lattice, destructing the spinel structure and releasing metallic ions.

Figure 5 also shows that adding dichromic acid significantly improves the leaching yield of Cr for all ores, which is mainly attributed to the strong oxidization potential of dichromic acid. When the dichromic acid/chromite ratio was 0.08, about 60% of the Cr was extracted from LFC, and the recovery rate of Cr in MFC and HFC tests were higher than 90%. The ion concentrations of leachate were analyzed by chemical analysis and ICP-OES analysis, also reported in Figure 5. Results show that no chromium ion besides the Cr^{3+} and Cr^{6+} was found in the filtrate. In test with LFC, the Cr(VI) concentration was $2.26 \text{ g}\cdot\text{L}^{-1}$, showing a little reduction in the leaching process. As for tests with MFC and HFC, very little Cr(VI) was detected in the leachates, and almost all of the iron ions occurred in the trivalent state. It may be speculated that the dichromic acid acts both as an oxidant and a catalyst in the decomposition of chromite. When the dichromic acid solution is used for treating low Fe(II)-chromite, the catalysis of dichromate ions plays a critical part on the chromite decomposition. The transformation of Cr(III) into Cr(IV) may firstly occur by Cr(VI) oxidizing causing the lattice distortion of spinel, and then the generated Cr(IV) transfers back to trivalent and hexavalent form via disproportionation due to the instability of Cr(IV). This could also explain why dichromic acid has less effect on the dissolution process of Fe(II)- and Cr(III)-free spinel, such as MgAl_2O_4 and MgFe_2O_4 [43]. On the basis of these findings, the proposed effects of dichromic acid have been illustrated in Figure 6.

The results suggest that dichromic acid is a suitable additive for sulfuric acid leaching of chromite, as it possesses a strong oxidizing capacity and can act as a catalyst. However, since the dichromic acid is consumed only by Fe(II), the dosage used for treating low Fe(II)-chromite should be carefully controlled. Moreover, a reduction treatment for reducing residual Cr(IV) is required to prevent the leaching products from containing Cr(IV)-rich phase. The Cr cycle during the leaching process of chromite is depicted in Figure 7.

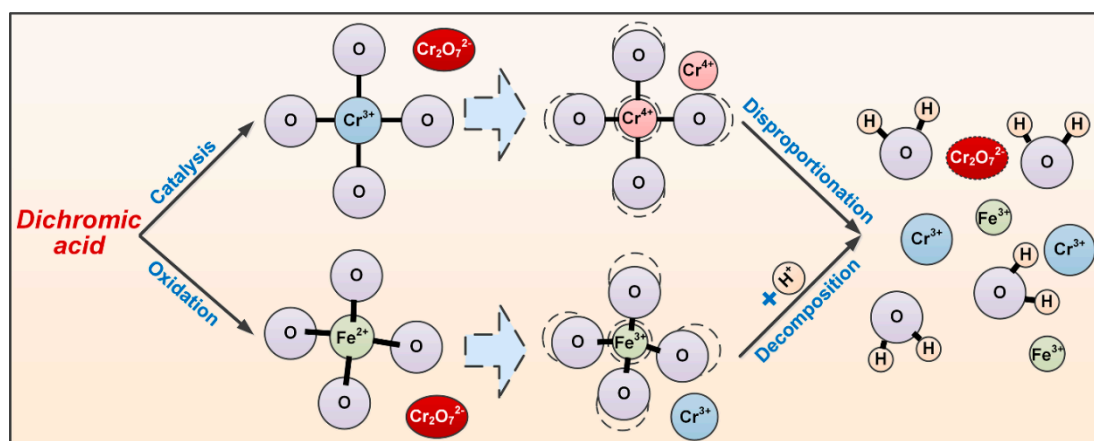


Figure 6. Illustration of the effects of dichromic acid on chromite decomposition.

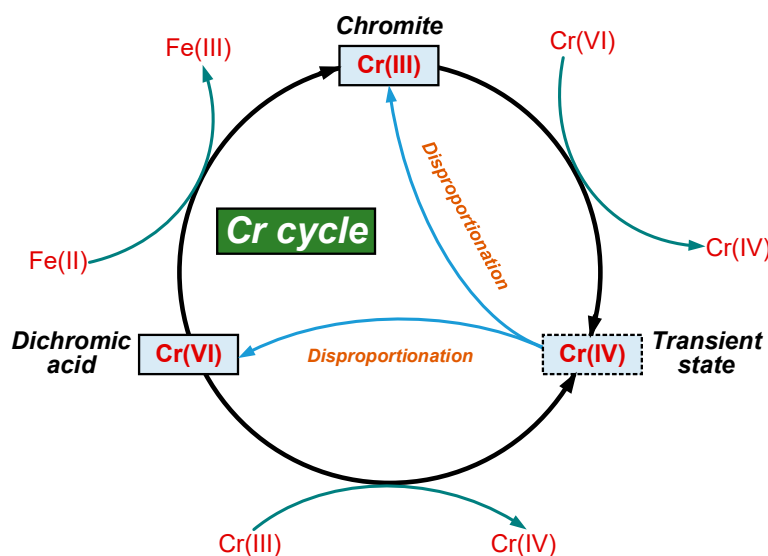


Figure 7. Cr cycle during the leaching process of chromite.

3.5. Product Preparation

A reducing treatment to transform residual Cr(IV) into Cr(III) is a necessary process before subsequent impurity separation. Scales stripped in the rolling process of steel sheets were collected and used as a reductant for the reducing treatment of the leachate. In the current work, solvent extraction by 2-ethylhexyl dihydrogen phosphate (P507) was conducted to accomplish the separation of Fe from the multi-element leachate. Some H_2O_2 was used and added in the leachate to oxidize Fe^{2+} to Fe^{3+} before P507 treating step. Afterwards, the P507 extractant was diluted with sulfonated kerosene in a volume ratio of 2:3 followed by a saponifying using 10 wt.% NaOH solution. The solvent extraction for leachate was conducted under atmospheric conditions five times to achieve a sufficient extraction of iron. The results showed that almost all of the iron could be recovered, and the Cr loss was less than 7%.

Metallic ions of Mg^{2+} and Al^{3+} in solution were recovered by subsequent oxalic acid and sodium hydroxide treatments. Figure 8 presents a flow sheet of the process for treating low-Fe(II) chromite proposed in this work. A product Cr_2O_3 was prepared from LFC by using the proposed process, with a chemical composition as follows: $\text{Cr}_2\text{O}_3\%$ = 99.36%, $\text{MgO}\%$ = 0.05%, and $\text{Al}_2\text{O}_3\%$ = 0.59%. The product can be used as a raw material for producing chrome pigment in China. A small amount of Al in the Cr_2O_3 pigment is beneficial for the color performance, so it is not necessary to fully remove Al from the product. All wastes discharged to the environment meet the Chinese discharge standard.

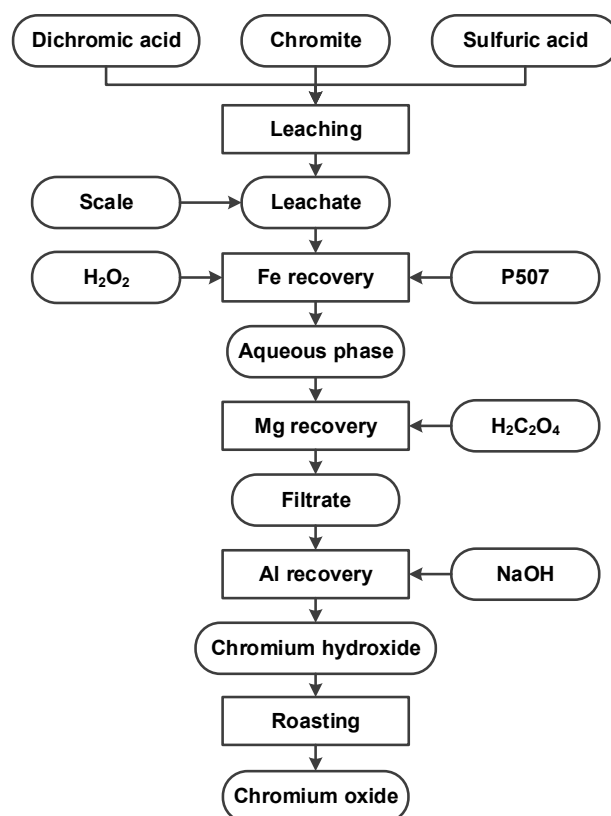


Figure 8. Flow sheet of the proposed process route for treating low-Fe(II) chromite.

4. Conclusions

To investigate the feasibility of sulfuric acid-based leaching of low Fe(II)-chromite, the optimal experimental conditions for leaching of a Zimbabwean chromite with 1.52% of FeO were determined by a Box–Behnken design (BBD). Second-order polynomial regression models capturing the functional relationships between the processing parameters (sulfuric acid concentration C , dichromic acid/chromite ratio r , and processing temperature T) and the extraction yields of Cr and Fe were proposed and validated. The significance of model terms was statistically evaluated, showing that C , r , Cr , C^2 and T^2 were significant terms for the Cr model, and C , r , T , CT , C^2 , r^2 , and T^2 for the Fe model. The dependent variables exhibited a strong inter-correlation of variables, and the prediction accuracy of the two models was excellent. Three-dimensional response surfaces were plotted to depict the overall and coupled effects of the leaching parameters on the extraction yield. Optimum conditions of the leaching process were found at a temperature of $T = 176$ °C, a dichromic acid/chromite ratio of $r = 0.12$, and a sulfuric acid concentration of $C = 81\%$.

Three chromites with various contents of Fe(II) were studied to investigate the dissolution behavior of chromite in sulfuric acid-based solution and the effect of dichromic acid. Results indicated that the decomposition efficiency of chromite strongly depended on the Fe(II) content. The dichromic acid acts both as an oxidant and a catalyst in the leaching process, and the catalysis plays a principal role on the decomposition of low Fe(II)-chromite. The Cr cycle during the leaching process of chromite was further illustrated.

Based on the findings of the work, a novel process for treating low-Fe(II) chromite by sulfuric acid-based leaching is proposed, and a chromium oxide is obtained as a product. No Cr-bearing wastes are discharged to the environment from this process, making it an interesting alternative for scale-up tests.

Author Contributions: Conceptualization, Q.Z. and P.S.; Funding acquisition, Q.Z. and L.S.; Methodology, C.L.; Investigation, Q.Z.; Writing—Original Draft Preparation, Q.Z.; Project administration, M.J.; Writing—Review & Editing, R.Z. and H.S. All authors have read and agreed to the published version of the manuscript.

Funding: This work was supported by The National Key Research and Development Program of China (No. 2017YFB0304603), the National Natural Science Foundation of China (No. 51704068), the Liaoning Provincial Natural Science Foundation of China (No. 2019-MS-127), and the Fundamental Research Funds for the Central Universities (No. N2025035 and N180725008).

Conflicts of Interest: The authors declare no conflict of interest.

Abbreviations

List of nomenclature and abbreviations.

TC	Turkish chromite
RSM	Response surface methodology
BBD	Box-Behnken design
C	Sulfuric acid concentration
<i>r</i>	Dichromic acid/chromite ratio
<i>T</i>	Processing temperature
ICP-OES	Inductively coupled plasma-optical emission spectrometry
LFC	low Fe(II)-chromite
MFC	Medium Fe(II)-chromite
HFC	High Fe(II)-chromite
XRD	X-ray diffraction
CSM	Crystallographica Search-Match
PDF	Powder Diffraction File
ICDD	International Centre for Diffraction Data
SEM-EDS	Scanning electron microscopy-energy-dispersive X-ray spectroscopy
ANOVA	Analysis of variance
R^2	Coefficient of determination
Adj. R^2	Adjusted coefficient of determination
Pred. R^2	Predicted coefficient of determination
R_{Cr}	Extraction yields of Cr
R_{Fe}	Extraction yields of Fe
$R_{Cr(exp)}$	Experimental extraction yields of Cr
$R_{Fe(exp)}$	Experimental extraction yields of Fe
C.V.%	Coefficients of variance

References

- Feng, H.; Li, H.B.; Jiang, Z.H.; Zhang, T.; Dong, N.; Zhang, S.C.; Han, P.D.; Zhao, S.; Chen, Z.G. Designing for high corrosion-resistant high nitrogen martensitic stainless steel based on DFT calculation and pressurized metallurgy method. *Corros. Sci.* **2019**, *158*, 108081. [[CrossRef](#)]
- Wu, Y.; Song, S.; Xue, Z.; Nath, M. Formation mechanisms and leachability of hexavalent chromium in Cr₂O₃-containing refractory castables of electric arc furnace cover. *Metall. Mater. Trans. B* **2019**, *50*, 808–815. [[CrossRef](#)]
- Zhao, Q.; Shao, Z.B.; Liu, C.J.; Jiang, M.F.; Li, X.T.; Zevenhoven, R.; Saxén, H. Preparation of Cu–Cr alloy powder by mechanical alloying. *J. Alloy. Compd.* **2014**, *607*, 118–124. [[CrossRef](#)]
- Koleli, N.; Demir, A. *Chromite. Environmental Materials and Waste*, 1st ed.; Prasad, M.N.V., Shih, K., Eds.; The Academic Press: Cambridge, UK, 2016; pp. 245–263. [[CrossRef](#)]
- Zhang, W. Demand analysis and prediction of world chrome resource. *Res. Ind.* **2016**, *18*, 87–91. (In Chinese) [[CrossRef](#)]
- Aktas, S.; Eyuboglu, C.; Morcali, M.; Özbey, S.; Sucuoglu, Y. Production of chromium oxide from Turkish chromite concentrate using ethanol. *High Temp. Mater. P-US.* **2015**, *34*, 237–244. [[CrossRef](#)]
- Morcali, M.H.; Eyuboglu, C.; Aktas, S. Synthesis of nanosized Cr₂O₃ from Turkish chromite concentrates with sodium borohydride (NaBH₄) as reducing agent. *Int. J. Miner. Process.* **2016**, *157*, 7–15. [[CrossRef](#)]

8. Zhang, Y.; Zheng, S.L.; Xu, H.B.; Du, H.; Zhang, Y. Decomposition of chromite ore by oxygen in molten NaOH–NaNO₃. *Int. J. Miner. Process.* **2010**, *95*, 10–17. [[CrossRef](#)]
9. Yarkadaş, G.; Yildiz, K. Effects of mechanical activation on the soda roasting of chromite. *Can. Metall. Quart.* **2013**, *48*, 69–72. [[CrossRef](#)]
10. Bolaños-Benítez, V.; Hullebusch, E.D.V.; Lens, P.N.L.; Quantin, C.; Vossenbergh, J.V.D.; Subramanian, S.; Sivry, Y. (Bio)leaching Behavior of Chromite Tailings. *Minerals-Basel* **2018**, *8*, 261. [[CrossRef](#)]
11. Kumar, N.; Nagendran, R. Fractionation behavior of heavy metals in soil during bioleaching with *Acidithiobacillus thiooxidans*. *J. Hazard. Mater.* **2009**, *169*, 1119–1126. [[CrossRef](#)]
12. Wang, Y.S.; Pan, Z.Y.; Lang, J.M.; Xu, J.M.; Zheng, Y.G. Bioleaching of chromium from tannery sludge by indigenous *Acidithiobacillus thiooxidans*. *J. Hazard. Mater.* **2007**, *147*, 319–324. [[CrossRef](#)] [[PubMed](#)]
13. Hutchinson, T.H.; Williams, T.D.; Eales, G.J. Toxicity of cadmium, hexavalent chromium and copper to marine fish larvae (*Cyprinodon variegatus*) and copepods (*Tisbe battagliai*). *Mar. Environ. Res.* **1994**, *38*, 275–290. [[CrossRef](#)]
14. Beukes, J.P.; Preez, S.P.D.; Zyl, P.G.V.; Paktunc, D.; Fabritius, T.; Päätao, M.; Cramer, M. Review of Cr(VI) environmental practices in the chromite mining and smelting industry-Relevance to development of the Ring of Fire, Canada. *J. Clean. Prod.* **2017**, *165*, 874–889. [[CrossRef](#)]
15. Looock-Hattingh, M.M.; Beukes, J.P.; Zyl, P.G.V.; Tiedt, L.R. Cr(VI) and conductivity as indicators of surface water pollution from ferrochrome production in South Africa: Four case studies. *Metall. Mater. Trans. B* **2015**, *46*, 2315–2325. [[CrossRef](#)]
16. Peralta, R.J.; Gardea-Torresdey, L.J.; Tiemann, J.K.; Gomez, E.; Arteaga, S.; Rascon, E.; Parsons, G.J. Uptake and effects of five heavy metals on seed germination and plant growth in alfalfa (*Medicago sativa* L.). *B. Environ. Contam. Toxicol.* **2001**, *66*, 727–734. [[CrossRef](#)]
17. Li, J.L.; Mou, Q.Q.; Zeng, Q.; Yue, Y. Experimental study on precipitation behavior of spinels in stainless steel-making slag under heating treatment. *Processes* **2019**, *7*, 487. [[CrossRef](#)]
18. Zeng, Q.; Li, J.L.; Mou, Q.Q.; Zhu, H.Y.; Xue, Z.L. Effect of FeO on spinel crystallization and chromium stability in stainless steel-making slag. *JOM* **2019**, *71*, 2331–2337. [[CrossRef](#)]
19. Liao, C.Z.; Tang, Y.Y.; Lee, P.H.; Liu, C.S.; Shih, K.M.; Li, F.B. Detoxification and immobilization of chromite ore processing residue in spinel-based glass-ceramic. *J. Hazard. Mater.* **2017**, *321*, 449–455. [[CrossRef](#)]
20. Nath, M.; Song, S.; Garbers-Craig, A.M.; Li, Y. Phase evolution with temperature in chromium-containing refractory castables used for waste melting furnaces and Cr(VI) leachability. *Ceram. Int.* **2018**, *44*, 20391–20398. [[CrossRef](#)]
21. Zhao, Q.; Liu, C.J.; Cao, L.H.; Jiang, M.F.; Li, B.K.; Saxén, H.; Zevenhoven, R. Shear-force based stainless steel slag modification for chromium immobilization. *ISIJ Int.* **2019**, *59*, 583–589. [[CrossRef](#)]
22. Zhao, Q.; Liu, C.J.; Gao, T.C.; Gao, L.; Saxén, H.; Zevenhoven, R. Remediation of stainless steel slag with MnO for CO₂ mineralization. *Process Saf. Environ.* **2019**, *127*, 1–8. [[CrossRef](#)]
23. Geelhoed, J.S.; Meeussen, J.C.L.; Roe, M.J.; Hillier, S.; Thomas, R.P.; Farmer, J.G.; Paterson, E. Chromium remediation or release? Effect of iron(II) sulfate addition on chromium(VI) leaching from columns of chromite ore processing residue. *Environ. Sci. Technol.* **2003**, *3*, 3206–3216. [[CrossRef](#)] [[PubMed](#)]
24. Graham, M.C.; Farmer, J.G.; Anderson, P.; Paterson, E.; Hillier, S.; Lumsdon, D.G.; Bewley, R.J.F. Calcium polysulfide remediation of hexavalent chromium contamination from chromite ore processing residue. *Sci. Total. Environ.* **2006**, *364*, 32–44. [[CrossRef](#)] [[PubMed](#)]
25. Su, C.; Ludwig, R.D. Treatment of hexavalent chromium in chromite ore processing solid waste using a mixed reductant solution of ferrous sulfate and sodium dithionite. *Environ. Sci. Technol.* **2005**, *39*, 6208–6216. [[CrossRef](#)] [[PubMed](#)]
26. Zhao, Q.; Liu, C.J.; Shi, P.Y.; Zhang, B.; Jiang, M.F.; Zhang, Q.S.; Zevenhoven, R.; Saxén, H. Sulfuric acid leaching kinetics of South African chromite. *Int. J. of Miner. Metall. Mater.* **2015**, *22*, 233–240. [[CrossRef](#)]
27. Jiang, M.F.; Zhao, Q.; Liu, C.J.; Shi, P.Y.; Zhang, B.; Yang, D.P.; Saxén, H.; Zevenhoven, R. Sulfuric acid leaching of South African chromite. Part 2: Optimization of leaching conditions. *Int. J. Miner. Process.* **2014**, *130*, 102–107. [[CrossRef](#)]
28. Zhao, Q.; Liu, C.J.; Shi, P.Y.; Zhang, B.; Jiang, M.F.; Zhang, Q.S.; Saxén, H.; Zevenhoven, R. Sulfuric acid leaching of South African chromite. Part 1: Study on leaching behavior. *Int. J. Miner. Process.* **2014**, *130*, 95–101. [[CrossRef](#)]

29. Zhang, B.; Shi, P.Y.; Jiang, M.F. Advances towards a clean hydrometallurgical process for chromite. *Miner. Basel* **2016**, *6*, 7. [[CrossRef](#)]
30. Liu, C.J.; Qi, J.; Jiang, M.F. Experimental study on sulfuric acid leaching behavior of chromite with different temperature. *Adv. Mater. Res.* **2011**, 361–363, 628–631. [[CrossRef](#)]
31. Zhao, Q.; Liu, C.J.; Yang, D.P.; Shi, P.Y.; Jiang, M.F.; Li, B.K.; Saxén, H.; Zevenhoven, R. A cleaner method for preparation of chromium oxide from chromite. *Process Saf. Environ.* **2017**, *105*, 91–100. [[CrossRef](#)]
32. Biermann, W.J.; Heinrichs, M. The attack of chromite by sulphuric acid. *Can. J. Chem.* **1960**, *38*, 1449–1454. [[CrossRef](#)]
33. Geveci, A.; Topkaya, Y.; Ayhan, E. Sulfuric acid leaching of Turkish chromite concentrate. *Miner. Eng.* **2002**, *15*, 885–888. [[CrossRef](#)]
34. Vardar, E.; Eric, R.H.; Letowski, F.K. Acid leaching of chromite. *Mine. Eng.* **1994**, *7*, 605–617. [[CrossRef](#)]
35. Das, D.; Vimala, R.; Das, N. Biosorption of Zn(II) onto *Pleurotus platypus*: 5-Level Box-Behnken design, equilibrium, kinetic and regeneration studies. *Ecol. Eng.* **2014**, *64*, 136–141. [[CrossRef](#)]
36. Jeganathan, P.M.; Venkatachalam, S.; Karichappan, T.; Ramasamy, S. Model development and process optimization for solvent extraction of polyphenols from red grapes using Box-Behnken design. *Prep. Biochem. Biotech.* **2014**, *44*, 56–67. [[CrossRef](#)] [[PubMed](#)]
37. Zhao, Q.; Shao, Z.B.; Leng, Q.C.; Zhang, X.D.; Liu, C.J.; Li, B.K.; Jiang, M.F. Preparation of Cu–Cr alloy powder by heat mechanical alloying and Box-Behnken design based optimization. *Powder Technol.* **2017**, *321*, 326–335. [[CrossRef](#)]
38. Zhao, Q.; Liu, C.J.; Li, B.K.; Zevenhoven, R.; Saxén, H.; Jiang, M.F. Recovery of chromium from residue of sulfuric acid leaching of chromite. *Process Saf. Environ.* **2018**, *113*, 78–87. [[CrossRef](#)]
39. Vaari, J. Molecular dynamics simulations of vacancy diffusion in chromium(III) oxide, hematite, magnetite and chromite. *Solid State Ion.* **2015**, *270*, 10–17. [[CrossRef](#)]
40. Mourabet, M.; El Rhilassi, A.; El Boujaady, H.; Bennani-Ziatni, M.; El Hamri, R.; Taitai, A. Removal of fluoride from aqueous solution by adsorption on Apatitic tricalcium phosphate using Box-Behnken design and desirability function. *Appl. Surf. Sci.* **2012**, *258*, 4402–4410. [[CrossRef](#)]
41. Tathavakar, V.D.; Antony, M.P.; Jha, A. The physical chemistry of thermal decomposition of South African chromite minerals. *Metall. Mater. Trans. B* **2005**, *36*, 75–84. [[CrossRef](#)]
42. Wang, E.H.; Luo, C.; Chen, J.H.; Hou, X.M. High-performance chromite by structure stabilization treatment. *J. Iron Steel Res. Int.* **2020**, *27*, 167–179. [[CrossRef](#)]
43. Zhao, Q.; Liu, C.J.; Li, B.K.; Jiang, M.F. Decomposition mechanism of chromite in sulfuric acid-dichromic acid solution. *Int. J. Min. Met. Mater.* **2017**, *24*, 1361–1369. [[CrossRef](#)]



© 2020 by the authors. Licensee MDPI, Basel, Switzerland. This article is an open access article distributed under the terms and conditions of the Creative Commons Attribution (CC BY) license (<http://creativecommons.org/licenses/by/4.0/>).